CHAPTER II

LITERATURE REVIEW

2.1 SOIL CHARACTERIZATION FOR TRACTION MODELLING

For off-road vehicle engineering the measurement of the soil properties is one of the fundamental tasks for the prediction and evaluation of tractive performance. Performance evaluation of terrain-vehicle systems involves both the design parameters for the vehicle and the measurement and evaluation of the physical environment within which the vehicle operates. The soil mechanical properties can be categorized as soil physical properties and soil strength parameters.

Soil physical properties affect the tractive performance of a vehicle by changing the soil strength characteristics under different conditions. However, a universal standard method does not yet exist for the measurement of the specific soil parameters. The classification and the measurement of the soil physical properties therefore depend much on the requirements of the individual user.

By utilizing the basic concepts from geotechnical and civil engineering, Karafiath & Nowatzki (1978) quoted an extensive range of references, definitions and measurements of permanent and transient soil properties for off-road vehicle engineering. Among the soil physical properties described by Karafiath & Nowatzki (1978) and Koolen & Kuipers (1983), some are usually necessary for traction such as soil classification by composition, soil porosity, soil water content, and soil density.

When the vehicle travels over a soft terrain surface, soil strength parameters are the major factors affecting the supporting, floating, shear, friction and other abilities of the soil under the vehicle load. The prediction of off-road vehicle performance, to a large

extent, depends on the proper evaluation and measurement of the strength parameters of the terrain which has been one of the major objectives of terrain-vehicle mobility research.

In geotechnical engineering, the standard methods for measuring soil strength parameters usually involve laboratory experiments, carried out on relatively small soil samples. In off-road vehicle engineering, if the soil strength and deformation characteristics are to be closely related to the field conditions under which the performance of the vehicles are evaluated, it is essential to measure the soil parameters in the field. The techniques currently in use for measuring and characterizing in-situ soil strength properties including the cone penetrometer (ASAE, 1988), bevameter (Bekker, 1969; Wong, 1993) and other techniques (Chi, Tessier, McKyes & Laguë, 1993), adopted from civil engineering.

In the highly theoretical models, utilizing the elastic-plastic theory and the finite element method (Chi, Kushwaha & Shen, 1993; Shen & Kushwaha, 1998), the soil parameters are usually measured by laboratory experiments, adapted from civil engineering such as a triaxial test and a direct shear test. As much as eight parameters may need to be measured under laboratory conditions before the development of the model (Chi, Kushwaha & Shen, 1993). This probably is the reason why the purely theoretical methods have not been used extensively for practical applications. Therefore, for the in-situ measurement in the field, the cone penetrometer and bevameter techniques are still the two most frequently used for soil characterization for traction and mobility modelling.

2.1.1 The cone penetrometer technique for soil characterization

The cone penetrometer used to evaluate soil strength for trafficability studies was initially applied by the U.S. Army Engineer Waterways Experimental Station (WES) (Freitag, 1965). To interpret and compare the results, the design and use of the cone penetrometer for agricultural applications is standardized as ASAE S313.2 (ASAE,

1988). This ASAE standard also specifies the index application range for different penetrometer types, penetration speed and depth increments for soil characterization.

The penetrometer consists of a circular 30° stainless steel cone mounted on a circular stainless steel shaft as shown in Figure 2.1. Other standardized dimensions of the penetrometer and the components are also shown in Figure 2.1.

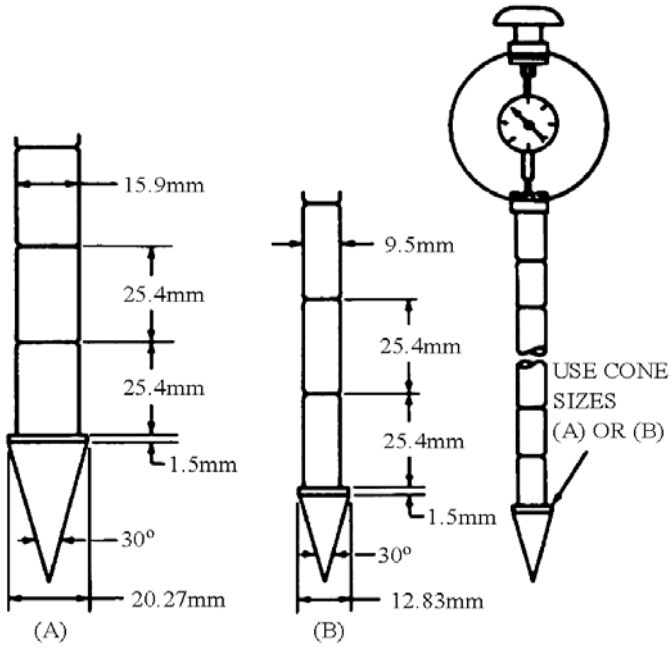

Figure 2.1. Cone penetrometer standardized by the ASAE S313.2.

The value of "Cone Index (CI)" represents the average penetration force per unit projected cone base area exerted by the soil upon the conical head when forced down to a specific depth at a penetration rate of about 3 cm/s as recommended by the ASAE standard S313.2 (ASAE, 1988). The cone index constitutes a compound parameter reflecting the comprehensive influence of shear, compression and even soil-metal friction.

The CI values may vary considerably with depth (Wismer & Luth, 1973). Therefore, the CI values usually used for traction prediction are the average value recorded over a depth corresponding to the maximum tyre or track sinkage.

For many years, the penetration test remained a very popularly used method applied by researchers for soil compaction and for some empirical traction studies. It is not only because of simplicity, convenience and ease of use, but also the provision of valuable information about the mechanical state of the soil. The value of such information can best be assessed when the CI is correlated to other information or parameters obtained from other test devices such as triaxial tests or the bevameter techniques. Although the CI value is important for soil characterization, it is questionable whether only the one value of CI is sufficient to represent the sophisticated phenomenon of soil reaction under vehicle traffic.

2.1.2 The bevameter technique for soil characterization

The bevameter technique, originally developed by Bekker (1956, 1960 and 1969) is well documented for characterizing soil strength and soil sinkage parameters relevant to tractive performance. Since a traction device or running gear applies both contact pressure and tangential stresses to the terrain surface to develop tractive effort, it seems reasonable to simulate the real phenomenon by applying loads in both directions. The bevameter technique attempts to represent this situation better than other currently available techniques (Wong, 1989, 1993).

The bevameter technique consists of:

- a plate sinkage test to determine the pressure-sinkage relationships of the soil; and
- a shear test to determine the in situ shear strength parameters of the soil.

A complete bevameter is illustrated schematically in Figure 2.2.

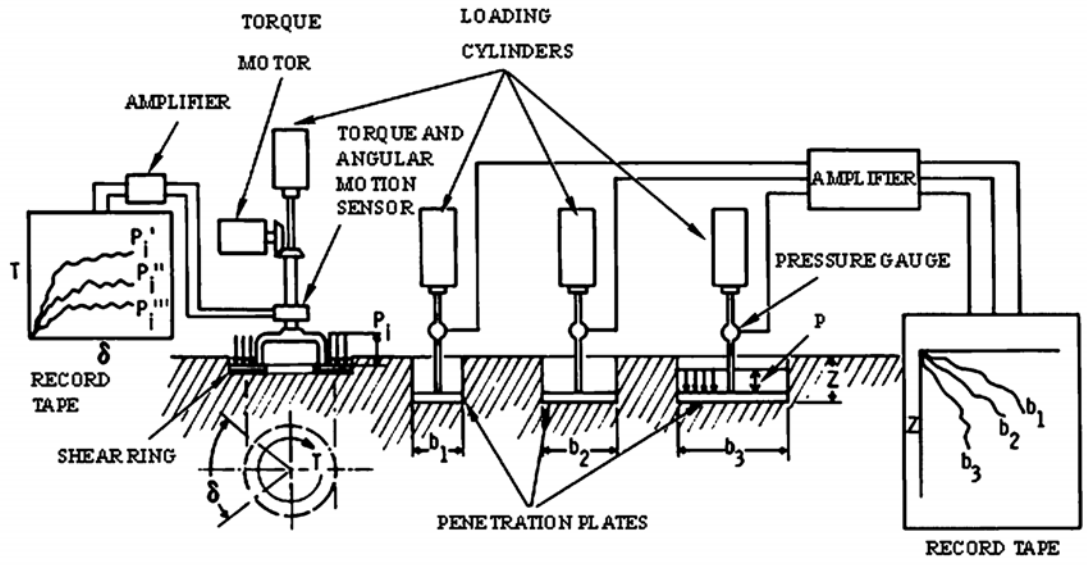

Figure 2.2. Schematic layout of a bevameter (Wong, 1993).

2.1.2.1 Measurement of pressure-sinkage relationships

By forcing rigid steel plates of different diameters or widths for rectangular plates into the soil surface for the specific test site, a typical family of pressure-sinkage curves can be generated as shown in Figure 2.3. In order to characterize the pressure-sinkage relationship for homogeneous terrain, the following equation was proposed by Bekker (1956):

$$p = (\frac{k_c}{b} + k_\phi)z^n \qquad (2.1)$$

where

p = contact pressure, (Pa).

b = width of a rectangular sinkage plate or radius of a circular sinkage plate, (m).

z = sinkage, (m).

k_c, k_ϕ and n = empirically determined pressure-sinkage soil characteristics.

In equation (2.1), k_c and k_ϕ have dimensional terms of N/m^{n+1} and N/m^{n+2} respectively and the parameters are related to soil cohesion and internal friction. The values of p and z are measured while the parameters k_c, k_ϕ and n are derived by fitting experimental data to the above equation (2.1) (Wong, 1989, 1993).

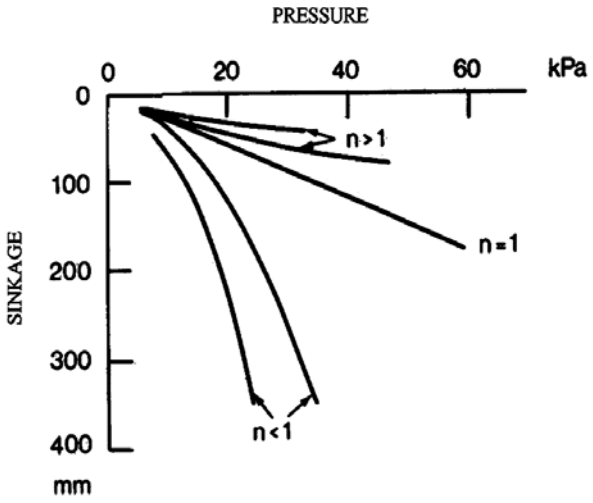

Figure 2.3. Typical pressure-sinkage curves (Bekker, 1969).

To obtain the parameters in equation (2.1), the results of a minimum of two tests with two plates having different widths or radii are required. The two tests produce two curves represented by two equations that can be rewritten in logarithmic form. They represent two parallel straight lines of the same slope on the log-log scale, where n is the slope of the lines. The values of k_c and k_ϕ are then calculated from the contact pressure for the two plates at z=1 (Wong, 1989).

It often happens that the pressure-sinkage curves may not be quite parallel on the log-log scale, probably due to the nonhomogeneity of the terrain and possible experimental errors. It is recommended by Wong (1989) that under the circumstances of two n values, the mean of the two values is usually accepted as the correct n value.

To improve the speed and efficiency of measurement and soil characterization for the bevameter technique, Wong (1980, 1989) developed a more rigorous and automated

data processing approach based on the weighted least squares method to derive the values of n, k_c and k_ϕ. In Wong's processing approach, the parameters in relation to repetitive pressure-sinkage loading-unloading were also taken into consideration. Although the technique improved the efficiency of obtaining k_c, k_ϕ and n, inherent problems still exist such as differences in behavior of a metallic plate compared to that of a rubber tyre or track, the effect of strain rate, speed of penetration and the fact that the plate can only characterize surface soil characteristics. The parameters k_c and k_ϕ in equation (2.1) also depend on the value of the exponent n.

To simplify equation (2.1) dimensionally, Reece (1965-1966) proposed the following alternative equation for the pressure-sinkage relationship:

$$p = (ck_c' + \gamma_s b k_\phi')\left(\frac{z}{b}\right)^n \tag{2.2}$$

where

k_c', k_ϕ' and n = dimensionless constants.

γ_s = unit weight of soil, (N/m^3).

c = soil cohesion, (Pa).

He also carried out a series of penetration tests to verify the validity of the principal features of the above equation. The sinkage plates used by Reece had various widths with aspect ratios of at least 4.5.

To measure the soil shear strength parameters, Reece (1965-66) built the apparatus as shown in Figure 2.4. One of the advantages of Reece's method and apparatus was that the sinkage caused by shear or so called slip-sinkage was also taken into consideration.

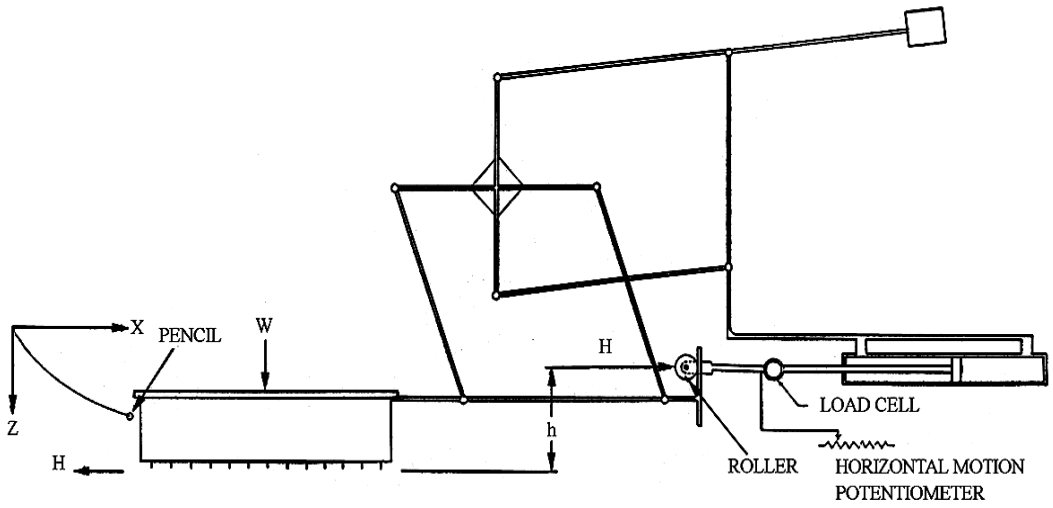

Figure 2.4. Reece's linear shear apparatus to measure soil shear strength and sinkage (Reece, 1965-1966).

Wong (1989) proved for various mineral terrains tested that the values of n, in both Bekker's equation and Reece's equation, were identical. It was also indicated that almost the same goodness-of-fit is resulted by fitting the same set of pressure-sinkage data with equation (2.1) or equation (2.2). Therefore, both Bekker's and Reece's equations were of similar form and comparable for the mineral terrain encountered for most operating conditions. As the bevameter technique was simpler and the parameters were easier to record and process, the bevameter method was more popularly used for traction studies.

Youssef and Ali (1982) reported that the accuracy of the plate sinkage analysis was affected by the size and shape of the plate used, as well as the soil strength parameters. They concluded that in order to achieve a more realistic result, the plate penetration rates ought to always be uniform and at a speed so as to simulate the situation under a track or a wheel. However, in practice, it was difficult to apply the load at such a high loading rate so as to simulate traffic. It was proved that the results from circular and rectangular sinkage plates were comparable.

Other researchers (Sela and Ehrlich, 1972; McKyes and Fan, 1985; Holm et al, 1987; Okello, 1991) also evaluated and investigated various pressure-sinkage relations for soil characterization. They were either very similar to Bekker's method or more complicated in processing than Bekker's method. Currently, the pressure-sinkage relationship, as proposed by Bekker, is still the popularly used expression for traction and is therefore chosen for the research.

2.1.2.2 Measurement of soil shear characteristics

Soil shear characterization is the second test constituting the bevameter technique. By the analysis of Bekker, a vehicle applies a shear to the terrain surface through its running gear, which results in the development of thrust and associated slip. To determine the shear strength of the terrain and to predict the tractive performance of an off-road vehicle, it is essential to measure the shear stress versus shear displacement relationship under various contact pressure conditions.

Bekker (1956) initially proposed the following equation to describe the shear stress versus shear displacement relationship for "brittle" soils with shear diagrams of a form similar to the aperiodic damped vibration:

$$\begin{aligned}\tau &= \frac{\tau_{\max}}{Y}\left(e^{(-K_2+\sqrt{K_2^2-1})K_1 j} - e^{(-K_2-\sqrt{K_2^2-1})K_1 j}\right) \\ &= \frac{c+\sigma\tan\phi}{Y}\left(e^{(-K_2+\sqrt{K_2^2-1})K_1 j} - e^{(-K_2-\sqrt{K_2^2-1})K_1 j}\right)\end{aligned} \tag{2.3}$$

where

τ = shear stress, (Pa).

τ_{max} = maximum shear stress, (Pa).

c = soil cohesion, (Pa).

ϕ = angle of soil internal shearing resistance, (degree).

σ = contact pressure, (Pa).

K_1, K_2 = empirical constants for soil shear.

j = shear displacement, (m)

Y = the maximum value of the expression within the bracket.

Based on the data for a large number of field shear tests on a variety of natural terrain surfaces, Wong (1989, 1993) concluded that three basic forms of shear stress-shear displacement relationships, which varied from Bekker's basic equation, were encountered.

A. The first type of the shear stress-shear displacement relationship exhibited the characteristics that the shear stress initially increased sharply and reached a "hump" of maximum shear stress at a particular shear displacement, and then decreased and approached a more or less constant residual value with a further increase in shear displacement (Figure 2.5). This type of shear curve may be expressed by:

$$\tau = \tau_{max} K_r \{1 + [\frac{1}{K_r(1-e^{-1})} - 1] e^{1-j/K_\omega}\} (1 - e^{-j/K_\omega}) \qquad (2.4)$$

where K_r is the ratio of the residual shear stress τ_r to the maximum shear stress τ_{max} and K_ω the shear displacement where the maximum shear stress τ_{max} occurs.

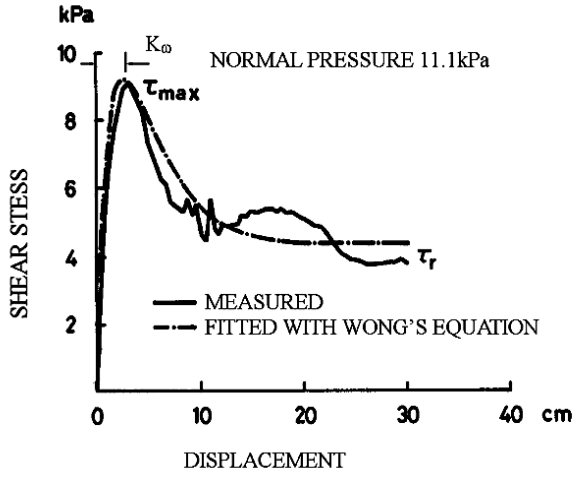

Figure 2.5. A shear curve exhibiting a peak and constant residual shear stress (Wong, 1989).

B. The second type of soil stress versus shear displacement relationship exhibited the characteristics that the shear stress increased with the shear displacement and reached a "hump" of maximum shear stress, and continued to decrease with a further increase in shear displacement as shown in Figure 2.6. It may be described by the following equation:

$$\tau = \tau_{max} (j / K_{\omega}) e^{1 - j / K_{\omega}} \tag{2.5}$$

where K_{ω} is the shear displacement where the maximum shear stress τ_{max} occurs. The rest of the symbols are as defined for equation (2.3).

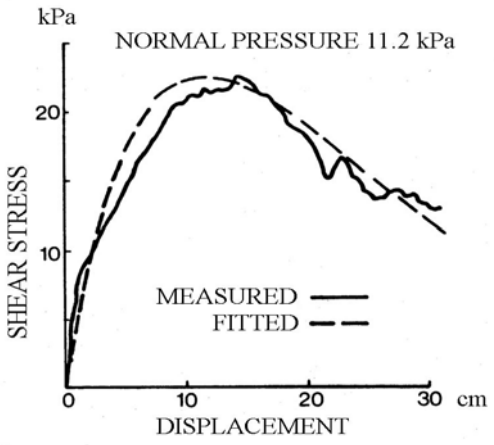

Figure 2.6. A shear curve exhibiting a peak and decreasing residual shear stress (Wong, 1989).

C. The third type of shear stress-shear displacement relationship was another modified version of Bekker's equation [equation (2.3)] containing only one constant. It was proposed by Janosi and Hanamoto (1961) as an exponential function. In practice, it is still the most popularly used expression.

$$\begin{aligned} \tau &= \tau_{max} (1 - e^{-j/K}) \\ &= (c + \sigma \tan \phi)(1 - e^{-j/K}) \end{aligned} \tag{2.6}$$

where K is referred to as the shear deformation modulus.

This relation did not display a hump but the shear stress increased with shear displacement and approached a constant value with a further increase in shear displacement as shown in Figure 2.7. The value of K determines the shape of the shear curve. Practically, the value of K can be measured directly from the shear curve or obtained from the calculation of the slope of the shear curve at the origin by differentiating τ with respect to j in equation (2.6):

$$\left.\frac{d\tau}{dj}\right|_{j=0} = \left.\frac{\tau_{\max}}{K} e^{-j/K}\right|_{j=0} = \frac{\tau_{\max}}{K} \tag{2.7}$$

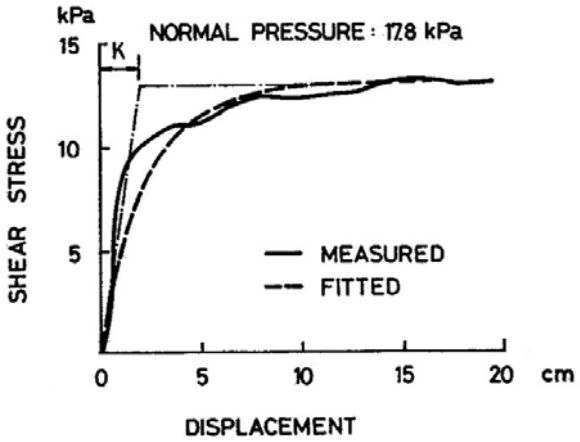

Figure 2.7. A shear curve exhibiting a simple exponential form (Wong, 1989).

The maximum shear stress for the curve is referred to as soil shear strength. The relation between the maximum shear stress and the corresponding contact pressure can be adequately described by the Mohr-Coulomb equation:

$$\tau_{\max} = c + \sigma \tan\phi \tag{2.8}$$

By plotting the measured values of the maximum shear stress versus the values of the corresponding applied contact pressure, a straight line may be obtained as shown in Figure 2.8. Therefore, the angle of soil internal shear ϕ and the soil cohesion c can be determined respectively by the slope of the straight line and the intercept of the straight line with the shear stress axis. Based on a large number of test results as shown

in Figure 2.8, Wills (1963) concluded that the shear strength parameters obtained from various shearing devices including the translational shear box, shear ring, rectangular shear plate, and rigid track were comparable.

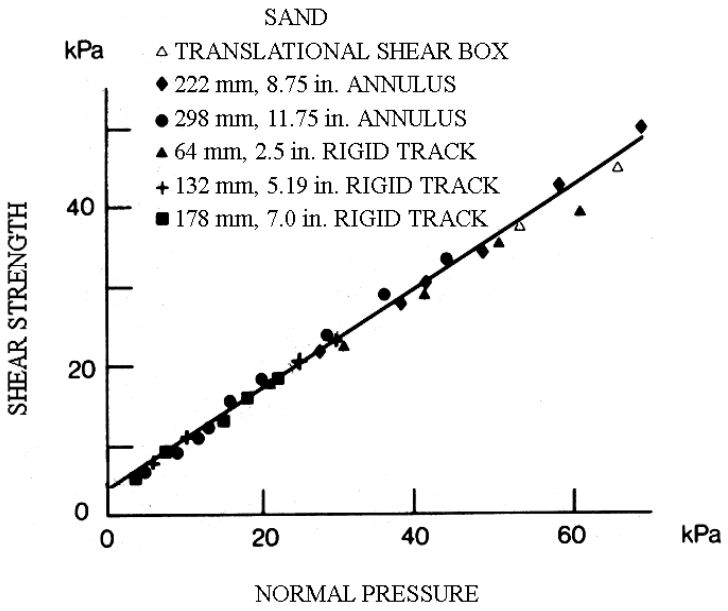

Figure 2.8. Shear strength of sand determined by various methods (Wills, 1963).

Summarized from the above literature review, it is obvious that the *in situ* measurement methods are preferable to the laboratory methods from the point of view of minimum disturbance of the soil sample. Furthermore, the *in situ* methods represent the real soil state in the field better than the methods of samples tested in a laboratory.

The cone penetrometer is perhaps the simplest in situ method and the most widely used technique. However, as only one parameter is used to describe the sophisticated phenomenon, the cone index is not sufficient to replace the soil strength parameters for representing the interaction between the running gear and the terrain surface. Despite its limitations to interpret the comprehensive soil property, the cone penetrometer with further modification and validation can efficiently be used for traction prediction. Alternatively it is also more suitable for the evaluation of soil compaction studies.

2.1.3 Friction and adhesion characterization for the soil-rubber contact surface

When a rubber tyre travels on a comparatively hard surface or a rubber track with a smooth surface travels on a terrain surface, minimal shear action occurs within the soil. The soil-rubber friction and the adhesion at the contact surface are the dominant factors for developing tractive thrust. Thus the characterization of rubber-soil friction and adhesion is of importance in developing a traction model for the track.

For describing the maximum friction and adhesion between a solid material surface and soil, the following equation, proposed by Terzaghi (1966), can be used:

$$\tau_{f\,max} = c_a + p\tan\delta \tag{2.9}$$

Where

τ_{fmax} = maximum friction stress, (Pa).
c_a = adhesion on the contact surface, (Pa).
p = normal pressure, (Pa).
δ = angle of friction between the rubber surface and soil, (degrees).

Equation (2.9) has the same form as equation (2.8), but the terms are different in physical definition.

Neal (1966) reported results of an investigation to compare the parameters in equations (2.8) and (2.9). As shown in Table 2.1, he concluded that the coefficient of soil to rubber friction, tan δ was, if not exactly the same, only slightly different from the coefficient of internal soil shear resistance, tan ϕ. However, the adhesion between rubber and soil c_a was less than the internal cohesion of the soil c, except for sand with both values negligibly small, which was not listed in the data. The value of c_a changed considerably with the soil water content. Reece's (1965-1966) research lead to the same conclusion as Neal's. This indicates that in sandy soils, where the values of rubber-soil friction coefficient are similar to the values of the coefficient of soil

internal shear resistance, the performance of a friction-based traction device is expected to be almost similar to that of shear-based traction device.

Table 2.1. Comparison of soil internal shear and soil-rubber frictional parameters (Neal, 1966).

Soil water content, %	Internal frictional angle for soil shear ϕ, degrees	Soil internal cohesion c, kPa	Soil-rubber frictional angle δ, degrees	Soil-rubber adhesion c_a, kPa
17.9	31.9	0.62	28.4	0.55
13.4	29.1	2.59	29.9	0.69
10.69	29.9	0.34	28.7	0.69
8.73	29.9	1.38	30.0	0.69

From the statistical data by Wong (1989), it was proved that the adhesion accounts for only a small portion of the total value of τ_{fmax}. Wong (1989) also concluded that among the soil shear parameters, although the specified test apparatus were not explained, the angles for soil-soil shearing resistance and rubber-soil friction were very similar, while the values of adhesion for rubber-soil were generally smaller than the soil-soil cohesion.

`

2.2 TRACTION PERFORMANCE MODELLING FOR WHEELED VEHICLES

2.2.1 Empirical methods for traction performance modelling

To predict the performance of vehicles, empirical methods are mainly based on the soil cone index (CI) as the single soil strength parameter to be measured. One of the well-known empirical models based on CI were originally developed during World War II by the US Army Waterways Experiment Station (WES) (Rula and Nuttall, 1971) as a means of measuring trafficability of terrain on a "go/no go" basis.

In developing the WES model (Rula and Nuttall, 1971), numerous tests were performed for a range of terrain types on primarily fine- and coarse-grained soils. The measured data for vehicle performance and terrain conditions were then empirically correlated, and a model known as the WES VCI was proposed for predicting vehicle performance on fine- and coarse-grained inorganic soils. The methods applied in the WES VCI models were very similar for wheeled and tracked vehicles (Rula and Nuttall, 1971).

With the widespread use of similitude and dimensional analysis in the early 1960's (Freitag, 1965; Turnage, 1972, 1978), an empirical model for the performance of a single tyre, based on dimensional analysis was developed at WES. In this model, two soil-tyre numerics, the clay-tyre numeric N_c and the sand-tyre numeric N_s were defined as below:

$$N_c = \frac{Cb_t d}{W} \times \left(\frac{\psi}{h}\right)^{1/2} \times \left(\frac{1}{1 + b_t / 2d}\right) \tag{2.10}$$

and

$$N_s = \frac{G(b_t d)^{3/2}}{W} \times \frac{\psi}{h} \tag{2.11}$$

where

b_t = tyre section width, (m).

CI = cone index, (Pa).

d = tyre diameter, (m).

h = tyre section height, (m).

W = tyre vertical load, (N).

G = sand penetration resistance gradient, (Pa/m).

ψ = tyre deflection, (m).

A soil-tyre numeric N_{cs} was proposed for cohesive-frictional soils by Wismer and Luth (1973) as:

$$N_{cs} = \frac{CIb_t d}{W} \tag{2.12}$$

The above mentioned three equations, especially equation (2.12), are the most commonly used empirical relationships to predict traction performance for wheels. On the bases of test results, mainly from soil bin tests in laboratories, the soil-tyre numerics were correlated with the three traction performance parameters for tyres. Among the parameters used in this equation, rolling resistance is a parameter often correlated with the soil-tyre numerics.

Wismer and Luth (1973) developed the following generally used equations for not highly compactible soils:

$$\rho = \frac{R_r}{W} = \frac{1.2}{N_{cs}} + 0.04 \tag{2.13}$$

$$\mu_g = \frac{T}{r_r W} = \frac{F_t}{W} = 0.75(1 - e^{-0.3 N_{cs} S}) \tag{2.14}$$

where

R_r = motion resistance, (N).

N_{cs} = wheel numeric, (CIbd/W).

T = applied torque, (Nm).

r_r = rolling radius based on a zero condition when net traction is zero at zero slip on a hard surface, (m).

F_t = gross tractive force, (N).

W = vertical load, (N).

ρ = motion resistance ratio.

μ_g = gross traction coefficient.

For the determination of r_r in the above equation, the slip is defined as:

$$i = (1 - \frac{V}{r\omega}) \times 100\% \tag{2.14a}$$

where

V = velocity of the wheel centre, (m/s).

r = radius of the wheel, (m).

ω = angular velocity, (rad/s).

Thus, the wheel pull coefficient or traction coefficient μ was calculated from:

$$\mu = \frac{F_t - R_r}{W} = \mu_g - \rho \tag{2.15}$$

For its simplicity and as only one parameter needed to be measured, the above described empirical method based on cone index used by many users to evaluate wheeled tractors under some given conditions. However, as pointed out by Wong (1989), the original concept of using the simple measurement of cone index is limited by the lack of information for the terrain conditions. The application is also strictly limited to cases which are similar to the conditions under which the original tests were undertaken. The exact range of soil conditions for which soil numerics are applicable also remains to be determined. This method should therefore be used with caution if the tyre or conditions differ from those under which the data were collected.

2.2.2 Analytical methods for traction performance modelling

Based on the parameters measured by the bevameter technique, Bekker originally developed one of the best known and most commonly used analytical methods - also known as a semi-empirical method for traction (Bekker, 1956, 1960, 1969; Wong, 1989, 1993). The principle of this analytical method was based on the assumptions that the vertical deformation in the soil under load was analogous to the soil deformation under a sinkage plate and that the shear deformation of the soil under a traction device was similar to the shear action performed by a rectangular or torsional shear device. The motion resistance of the running gear on a soft soil surface was predicted by assuming that the resistance was mainly caused by compacting the soil and the energy dissipated in forming a rut in the soil below the running gear. The total tractive effort was predicted by integrating the horizontal component of shear stress beneath the running gear in the direction of travel.

In the basic model proposed by Bekker (1956), a towed rigid wheel was analyzed based on the configuration of the contact surface as shown in Figure 2.9. For this simplified model, the motion resistance resulting from soil compaction was predicted as:

$$R_c = b_w \int_0^{Z_r} \left(\frac{k_c}{b} + k_\phi\right) z^n dz$$

$$= \frac{(3W)^{(2n+2)/(2n+1)}}{(3-n)^{(2n+2)/(2n+1)}(n+1)(k_c + b_w k_\phi)^{1/(2n+1)} D^{(n+1)/(2n+1)}} \qquad (2.16)$$

where

R_c = motion resistance, (N).

Z_r = depth of the rut, (m).

b_w = width of the wheel, (m).

W = wheel load, (N).

D = diameter of the wheel, (m).

k_c, k_ϕ and n = empirically determined pressure-sinkage soil characteristics.

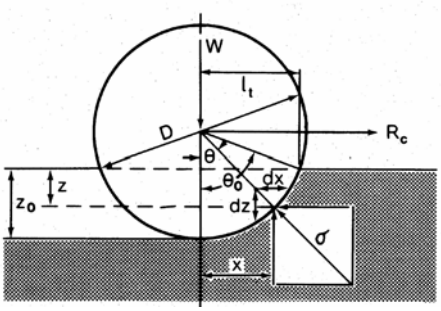

Figure 2.9. Simplified rigid wheel-soil interaction model by Bekker (1956).

This generalized equation is valid for moderate sinkage (i.e., $z_0 \leq D/6$) for any rigid wheel or highly inflated tyre with minimal deflection in homogeneous soft soils of any type. It is more accurate for larger wheel diameters and limited sinkage in soft soil. The sinkage of such a wheel z_0 is also determined from the following equation (Bekker, 1956):

$$z_0 = \left[\frac{3W}{(3-n)(k_c + b_w k_\phi)\sqrt{D}} \right]^{\frac{2}{2n+1}} \tag{2.17}$$

where

z_0 = sinkage of the wheel, (m).

b_w = width of the wheel, (m).

The rest of the symbols are as defined in equation (2.16).

For a pneumatic tyre, when the terrain is firm and the inflation pressure is sufficiently low, significant tyre deformation occurs (Figure 2.10). The sinkage of the tyre z_0 in this case can be determined by applying the following equation together with Bekker's sinkage equation:

$$z_0 = \left(\frac{p_{ti} + p_c}{(k_c / b_w) + k_\phi} \right)^{1/n} \tag{2.18}$$

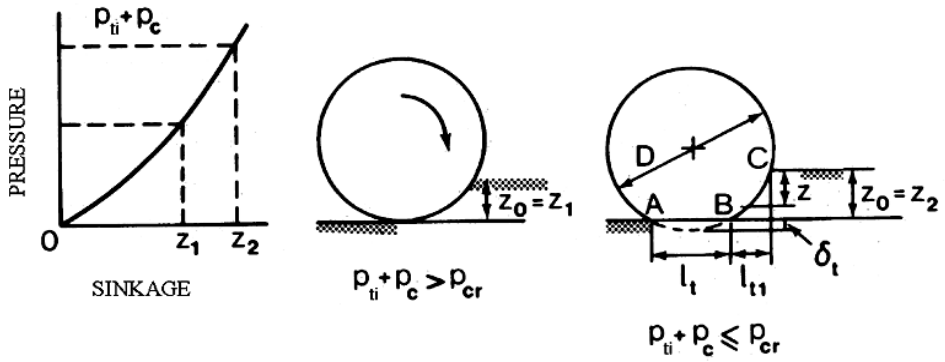

Figure 2.10. Deformation of a pneumatic tyre in different operating modes (Wong, 1989).

Under these circumstances, the motion resistance is given by:

$$R_c = \frac{b_w(p_{ti}+p_c)^{(n+1)/n}}{(n+1)(k_c/b_w+k_\phi)} \tag{2.19}$$

where

p_{ti} = inflation pressure, (Pa).

p_c = pressure due to the stiffness of the carcass, (Pa).

As proposed by Wong & Reece (1967), the analysis for the shear displacement developed along the contact area of a rigid wheel based on the analysis of the slip velocity V_j is shown in Figure 2.11 and is described by:

$$V_j = r\omega[1-(1-i)\cos\theta] \tag{2.20}$$

where

i = slip of the wheel as defined in equation (2.14a), (%).

r = wheel radius, (m).

ω = angular velocity of the wheel, (rad/s).

It is shown that the slip velocity for a rigid wheel varies with the angle θ and slip i.

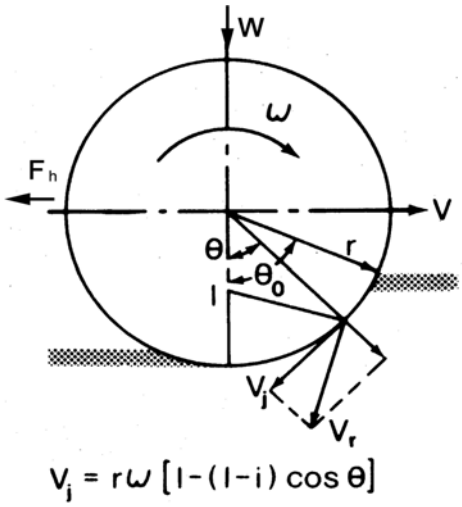

Figure 2.11. Analysis of shear displacement under a wheel (Wong, 1993).

The shear displacement along the interface is given by:

$$j = \int_0^t V_j dt = \int_0^{\theta_0} r\omega[1-(1-i)\cos\theta]\frac{d\theta}{\omega}$$
$$= r[(\theta_0 - \theta) - (1-i)(\sin\theta_0 - \sin\theta)] \qquad (2.21)$$

where θ_0 is the entrance angle of the wheel.

By applying the relationship of shear stress and shear displacement, as proposed by Janosi and Hanamoto (1961), the shear stress can be described as:

$$\tau(\theta) = [c + p(\theta)\tan\phi](1 - e^{j/K})$$
$$= [c + p(\theta)\tan\phi][1 - e^{-(r/K)[\theta_0 - \theta - (1-i)(\sin\theta_0 - \sin\theta)]}] \qquad (2.22)$$

By integrating the horizontal component of the stresses in the direction of travel over the entire contact area, the total tractive effort F_t can be determined:

$$F_t = \int_0^{\theta_0} \tau(\theta)\cos\theta d\theta \qquad (2.23)$$

To take into consideration the effect of shear stress on the vertical load and the effect of normal stress on the horizontal force, the equations for predicting the vertical load

and drawbar pull for a rigid wheel are given by equations (2.24) and (2.25) (Wong, 1993) respectively.

For vertical load,

$$W = rb_w \left[\int_0^{\theta_0} p(\theta) \cos \theta d\theta + \int_0^{\theta_0} \tau(\theta) \sin \theta d\theta \right] \quad (2.24)$$

For available pull,

$$F_h = rb_w \left[\int_0^{\theta_0} \tau(\theta) \cos \theta d\theta - \int_0^{\theta_0} p(\theta) \sin \theta d\theta \right] \quad (2.25)$$

Generally speaking, the methods for predicting the tractive performance for a pneumatic tyre are mainly dependent on the individual mode of operation. Other key issues for a wheel also include the distribution of normal and shear stress, and the profile of the contact patch.

2.3 TRACTION MODELLING FOR TRACKED VEHICLES

2.3.1 Empirical methods for traction performance modelling

Empirical methods are still playing an important role for the evaluation of the performance of tracked vehicles. The empirical methods are mainly based on cone penetrometer values as originally developed by WES (Rula and Nuttall, 1971). They follow similar methods used for the wheeled vehicles reviewed in the previous section.

2.3.2 Analytical methods for traction performance modelling

One of the most popular analytical methods for the performance of a track system was originally developed by Bekker (1956, 1960, 1969) based on the assumption that the track in contact with the terrain is similar to a rigid footing. By using Bekker's

pressure-sinkage equation (2.1), for a rigid, relatively smooth, uniformly loaded track, as shown in Figure 2.12, the track sinkage z_t is given by:

$$z_t = \left[\frac{p}{(k_c/b)+k_\phi}\right]^{1/n} = \left[\frac{W/bL}{(k_c/b)+k_\phi}\right]^{1/n} \tag{2.26}$$

The motion resistance of the track due to soil compaction R_c is:

$$R_c = \frac{1}{(n+1)(k_c/b+k_\phi)^{1/n}}\left(\frac{W}{L}\right)^{(n+1)/n} \tag{2.27}$$

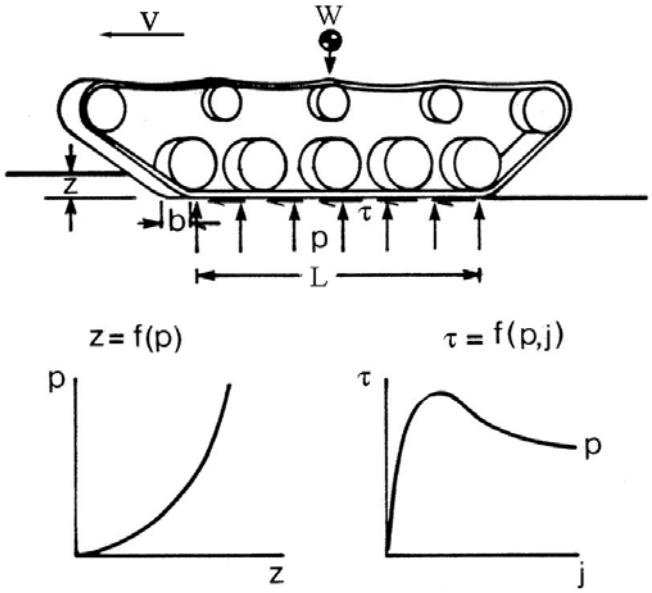

Figure 2.12. Simplified model for track-soil interaction (Wong, 1989).

If the contact pressure is uniformly distributed and the shear stress-shear displacement has a simple exponential relationship as shown in equation (2.6), the tractive effort of a track with contact area of A can be determined from:

$$\begin{aligned} F_t &= b\int_0^L (c + \frac{W}{bL}\tan\phi)(1 - e^{-ix/K})dx \\ &= (Ac + W\tan\phi)\left[1 - \frac{K}{iL}(1 - e^{-iL/K})\right] \end{aligned} \tag{2.28}$$

Using the maximum shear strength τ_{max} defined by equation (2.8), the maximum tractive effort F_{tmax} is therefore determined as:

$$\begin{aligned} F_{t\,max} &= A\,\tau_{max} \\ &= A[\,c + p\tan\phi\,] \\ &= Ac + W\tan\phi \end{aligned} \tag{2.29}$$

Thus the available pull F_h and the maximum pull F_{hmax} in horizontal direction are expressed by:

$$\begin{aligned} F_h &= F_t - R_c \\ &= (Ac + W\tan\phi)\left[1 - \frac{K}{iL}(1 - e^{-iL/K})\right] - \frac{1}{(n+1)(k_c/b + k_\phi)^{1/n}}\left(\frac{W}{L}\right)^{(n+1)/n} \end{aligned} \tag{2.30}$$

and

$$\begin{aligned} F_{h\,max} &= F_{t\,max} - R_c \\ &= (Ac + W\tan\phi) - \frac{1}{(n+1)(k_c/b + k_\phi)^{1/n}}\left(\frac{W}{L}\right)^{(n+1)/n} \end{aligned} \tag{2.31}$$

Practically, the distribution of normal stress on the track-terrain interface plays an important role for predicting the performance. In order to verify the theoretical assumption, Wills (1963) used a specially designed cantilever-type track link dynamometer to determine the distribution of normal pressure under a uniformly loaded rigid track by measuring the vertical and the horizontal forces between a track link and a track plate. The magnitude and distribution of horizontal shear force developed under the track were also measured. The effects of other different values of normal stress distribution (Figure 2.13) on tractive efforts were also investigated by Wills (1963).

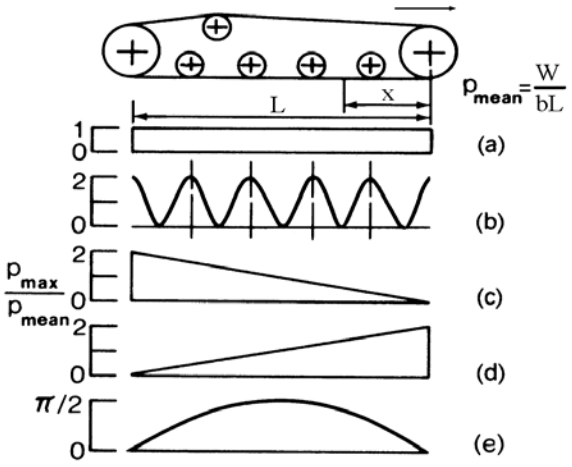

Figure 2.13. Various patterns of idealized contact pressure distribution under a track (Wills, 1963).

It proved that the normal stress distribution beneath a rigid track influenced the development of the tractive effort. In the case as shown in Figure 2.13(b), the normal pressure p has a multi-peak sinusoidal distribution expressed by:

$$p = \frac{W}{bL}\left(1 + \cos\frac{2n_p\pi x}{L}\right) \tag{2.32}$$

where n_p is the number of periods as shown in Figure 2.13. In a frictional soil with c=0, the shear stress developed along the contact length is expressed by:

$$\tau = \frac{W}{bL}\tan\phi\left(1+\cos\frac{2n_p\pi x}{L}\right)(1-e^{-ix/K}) \tag{2.33}$$

and the tractive effort is calculated as:

$$\begin{aligned} F_t &= b\int_0^L \frac{W}{bL}\tan\phi\left(1+\cos\frac{2n_p\pi x}{L}\right)(1-e^{-ix/K})dx \\ &= W\tan\phi\left[1+\frac{K}{iL}(e^{-iL/K}-1)+\frac{K(e^{-iL/K}-1)}{iL(1+4n_p{}^2K^2\pi^2/i^2L^2}\right] \end{aligned} \tag{2.34}$$

The tractive effort of a track with other contact pressure distribution patterns can be also predicted in a similar way. In the case of (c) (Figure 2.13), the pressure increases linearly from front to rear p=2[W/(bL)](x/L), and the tractive effort of a track in frictional soil is given by:

$$F_t = W\tan\phi\left[1-2\left(\frac{K}{iL}\right)^2\left(1-e^{-iL/K}-\frac{iL}{K}e^{-iL/K}\right)\right] \tag{2.35}$$

In the case of a contact pressure increasing linearly from rear to front, represented by p=2[W/(bL)](l-x)/L) as shown in Figure 2.13(d), the tractive effort of a track in frictional soil is calculated from:

$$F_t = 2W\tan\phi\left[1-\frac{K}{iL}\left(1-e^{-iL/K}\right)\right] - W\tan\phi\left[1-2\left(\frac{K}{iL}\right)^2\left(1-e^{-iL/K}-\frac{iL}{K}e^{-iL/K}\right)\right] \tag{2.36}$$

In the case of a sinusoidal distribution with maximum pressure at the center and zero pressure at the front and rear end (p=(W/bL)(π/2)sin(πx/L), as in Figure 2.13(d)), the tractive effort in a frictional soil is determined by:

$$F_t = W\tan\phi\left[1-\frac{e^{-iL/K}+1}{2(1+i^2L^2/\pi^2K^2)}\right] \tag{2.37}$$

Figure 2.14 shows the variation of the tractive effort with slip of a track with various types of contact pressure distribution on sand, as mentioned above (Wills, 1963). It can be seen that the contact pressure distribution has a noticeable effect on the development of tractive effort, particularly at low values of slip when the tractor is usually operated. In this point of view, the bottom one of the pressure distribution patterns as shown in the figure is most preferred for larger value of drawbar pull at lower value of slip. In fact, the distribution of normal pressure and shear stress are among the most important issues in the analytical models based on Bekker's method.

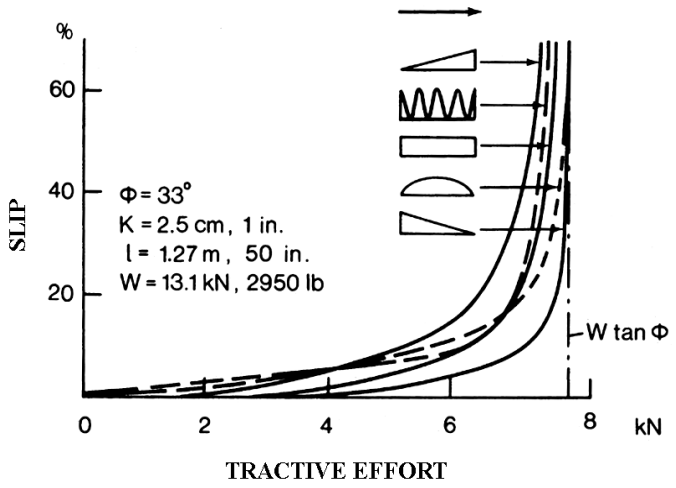

Figure 2.14. Effect of contact pressure distribution on the tractive performance of a track in sand (Wills, 1963).

The experiments performed and the results obtained by Wills (1963) in the laboratory with full size rigid tracks are important because in these experiments both the vertical and the horizontal forces acting on a track link were measured simultaneously. However, due to the practical difficulties to mount force transducers onto a track, little effort has since been made to measure the normal and horizontal forces simultaneously on the track. Other experiments aimed at the determination of the pressure distribution under tracks were only restricted to the measurement of normal stresses.

Wong (1989, 1993) developed a model based on the analysis of track-terrain interaction to predict the performance of the traditional steel track. In Wong's model, the contact pressure distribution was predicted by determining the shape of the deflected track in contact with the terrain. In the analysis, the track is assumed to be equivalent to a flexible belt and the assumed track-road wheel system travelling on a deformable terrain under steady-state conditions is shown in Figure 2.15. The magnitude of the slip velocity V_j of a point P on a flexible track is expressed by:

$$\begin{aligned} V_j &= V_t - V\cos\alpha \\ &= r\omega - r\omega(1 - i)\cos\alpha \\ &= r\omega[1 - (1 - i)\cos\alpha] \end{aligned} \tag{2.38}$$

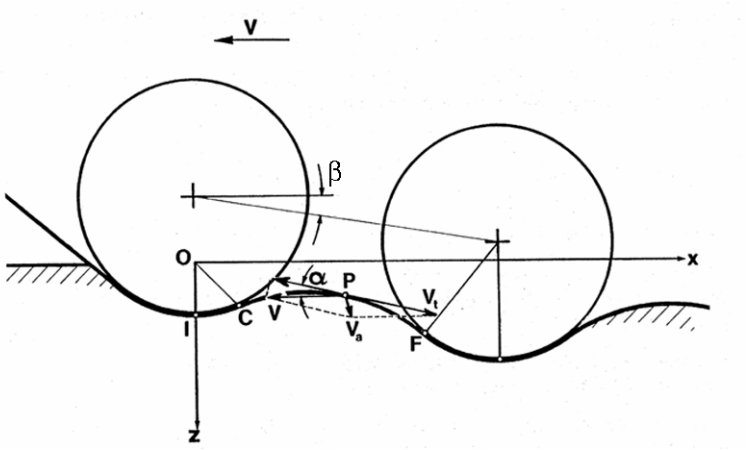

Figure 2.15. Deformation of the interaction surface used in Wong's model (Wong, 1993).

The shear displacement j along the track-terrain interface for contact length is given by:

$$\begin{aligned} j &= \int_0^t r\omega\,[\,1-(\,1-i\,)]\,dt \\ &= \int_0^{\ell} r\omega\,[\,1-(\,1-i\,)]\,\frac{d\ell}{r\omega} \\ &= \ell - (1-i)x \end{aligned} \tag{2.39}$$

The shear stress distribution is expressed by:

$$\tau(x) = [\,c + p(x)\tan\phi\,]\left\{1-\exp\left[-\left(\frac{\ell-(1-i)x}{K}\right)\right]\right\} \tag{2.40}$$

where p(x) is the contact pressure on the track and is a function of x.

In this model, for a vehicle with two tracks, the external motion resistance R_e is given by

$$R_e = 2b\int_0^{\ell_t} p\,\sin\,\alpha\,d\ell \tag{2.41}$$

And the tractive effort F_t for a vehicle with two tracks is given by:

$$F_t = 2b\int_0^{\ell_t} \tau \cos\alpha d\ell \tag{2.42}$$

In Wong's model, the response to repetitive loading was also included in the analysis.

According to the reported results, a close agreement between the measured and predicted contact pressure distribution values as well as drawbar performance was recorded.

It was mentioned by Wong (1993) that for a track with rubber pads, the part of the tractive effort generated by rubber-terrain interaction could be predicted by taking into consideration the portion of the vehicle weight supported by the rubber pads, the area of the rubber pads in contact with the terrain, and the characteristics of rubber-terrain frictional slip. However, there was no further description given in this respect.

2.4 DEVELOPMENT OF AND TRACTION CHARACTERISTICS FOR RUBBER TRACKS

Initially, the idea of rubber tracks was proposed in the early 1970's. The first type was a pneumatic rubber track tested by Taylor and Burt (1973). The pneumatic rubber track consisted of a circular shaped, and nylon reinforced flexible tyre, mounted over stretching wheels fixed to a frame. In their study, the traction performance and soil compaction was compared for a steel track, a pneumatic rubber track and a pneumatic tyre in a soil tank. The tractive efficiencies for various soil types ranged from 80% to 85% for both the steel and the pneumatic rubber tracks and from 55% to 65% for the pneumatic tyre. Maximum tractive efficiencies occurred at less than 10% slip for the tracks and between 15% and 25% for the tyre. In general, both the steel and pneumatic tracks had comparable traction performance characteristics. However, the performance of both tracks was much higher than that for a pneumatic tyre.

Evans and Gove (1986) reported the test results comparing the tractive performance and soil compaction for a rubber belt track and a four-wheel drive tractor. The tests were conducted in tilled soil and firm soil and proved that the rubber belt tractor, in comparison to the four-wheel drive tractor, developed higher tractive efficiencies at a specified pull ratio and generated an equivalent drawbar pull at lower slip levels. The maximum tractive efficiency in tilled and firm soil was 85% and 90% for the rubber belt tractor and 70% and 85% for the four-wheel drive tractor. The reported results for soil compaction tests conducted in the tilled soil showed that the rubber belt tractor and the four-wheel drive tractor caused similar increases in cone penetration resistance as they had equal mass. However, the measurement of subsoil pressure proved that at the same depth, peak subsoil vertical stresses were twice as high for the four-wheel drive tractor as for the rubber belt tractor. The rubber track also depicted a more uniformly distributed contact pressure under the track than for the wheel.

Culshaw (1988) reported about two experiments in which the tractive performance of rubber tracks were compared to that of tractor drive tyres. The first experiment was a comparison between a friction drive rubber track and a conventional radial type tractor tyre. The tests were conducted by alternatively mounting the track and the tyre on a single wheel tester. The results proved that the rubber track produced about 25% more drawbar pull than the tyre. The second experiment was a comparison between a small dumping truck running on rubber tracks and a conventional two-wheel drive tractor with a similar mass. It was proved that the truck produced twice the pull of the wheeled tractor with similar tractive efficiencies and caused less rutting on a soft soil.

Esch, Bashford, Von Bargen and Ekström (1990) reported a comprehensive traction performance comparison between a rubber belt track tractor and a four-wheel drive tractor equipped with dual wheels, having comparable power and mass. The drawbar tests were performed on four ground surface conditions: untilled oats stubble, disked oats stubble, plowed oats stubble, and maize stubble. The tractive performance was compared based on relationships of dynamic traction ratio to slip, tractive efficiency to slip and tractive efficiency to dynamic traction ratio. It showed that the rubber belt

track offered small advantages over the four-wheel drive tractor on firm surface but significant advantages under soft surface conditions.

In the research reported by Okello et al (1994), it was found that the rubber tracks had higher rolling resistance than the tractor driving wheel tyre apparently due to the internal power losses in the track unit. Accordingly, the tractive efficiencies of the rubber tracks were lower than that of the tyre because of the higher rolling resistance for the track.

Dwyer et al (1993) reviewed the research on rubber tracks at the Silsoe Research Institute. Two mathematical models, namely an infinitely stiff and infinitely flexible track (Figure 2.16), were described for predicting the tractive performance. The contact pressure at each point on the ground contact surface was calculated from the pressure-sinkage relationship in equation (2.1). The shear stress-shear displacement relationship in equation (2.6) was applied to predict the tangential stress. The equations of equilibrium were established by using the track deformation assumptions for two extreme flexibility situations. The equilibrium equations for the infinitely stiff model are as follow:

In the vertical direction:

$$W = b\int_0^L (p\cos\beta + \tau\sin\beta)dx \tag{2.43}$$

In the horizontal direction:

$$R_r = b\int_0^L p\sin\beta dx \tag{2.44}$$

and

$$F_t = b\int_0^L (\tau\cos\beta - p\sin\beta)dx \tag{2.45}$$

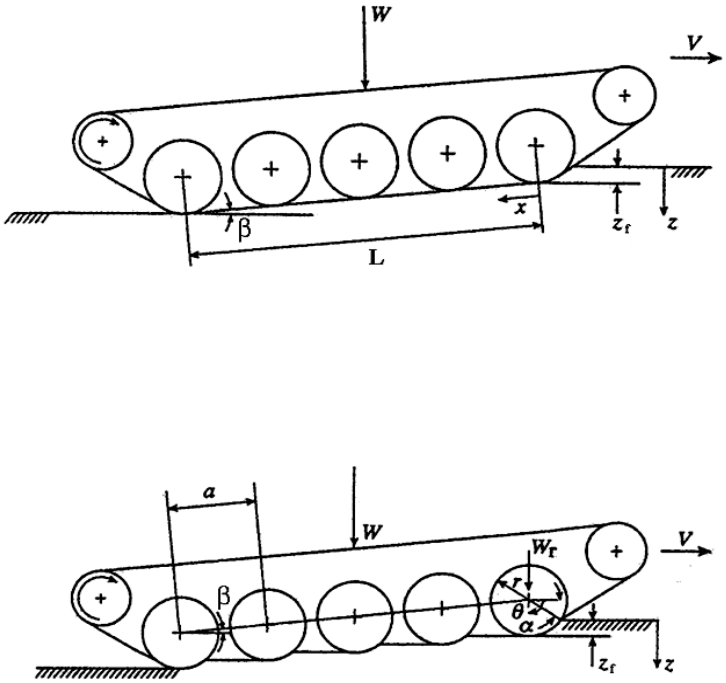

Figure 2.16. The infinitely stiff and the infinitely flexible models by Dwyer *et al.* (1993).

With the infinitely stiff assumption, the solution was independent of the diameter or spacing of the ground rollers and the ground contact area was a flat and rectangular plate. With the infinitely flexible model, the track unit behaved like a multi-wheel vehicle, as if there was no track at all, and the performance depended entirely on the number and diameter of the ground rollers. The results of the field tests with the experimental track unit on a single-wheel tester proved that the tractive performance of the rubber track was over-predicted by the infinitely stiff model and considerably under-predicted by the infinitely flexible model. The method, based on Wong's procedure, was used in the analysis. They determined that the profile of ground contact surface and thus the stress distribution was the major factor causing the difference.

A model was developed by Okello et al (1998) to study the traction performance and ground pressure distribution of a rubber track unit on soft agricultural soils. By closely following Wong's method of steel tracks, the model made use of relevant soil characterization parameters obtained by applying shear and sinkage tests based on the

bevameter technique. The effect of repetitive loading was also taken into consideration by the procedure suggested by Wong (1989). For their research a rubber track unit was mounted on a structure similar to the one for a traditional steel track. The theoretical model was validated against the experimental results by attaching the rubber track unit to the rear of a single-wheel tester. For two of the four soil conditions tested, the results from the theoretical prediction and the experimental data were compared and showed close agreement with a maximum difference of only 7.5%. For other two soil conditions, the predicted results were not provided for the reason of failed soil shear tests.

In recent years, the rubber tracks became more popular for their combined advantages when compared to conventional steel tracks and the wheels, as summarized in Chapter 1. The rubber tracks are currently mainly used on agricultural tractors and some construction machinery. However, they are also used on combines.

After the development over a decade, the Challenger tractor series equipped with rubber belt tracks from Caterpillar became the major rubber track crawler tractors available on the market. The historical development and the technical features for the Challenger Series were reported in the relevant ASAE lectures (Caterpillar Inc., 1995). A friction drive is utilized to transmit the power from the sprocket to the rubber belt tracks and the rubber tracks have lugs in contact with soil to generate the thrust effort.

According to the design principle, if the track tension is set higher than the maximum traction effort developed by the track, slip will not occur between the track and the driving wheel and the efficiency will not be reduced. Overloading of friction drives may lead to slipping of the rubber belt, but with minimal belt damage. However, a combination friction/positive drive unit leads to a longer service life for the rubber belt and positive safe transmission of driving power (Dudzinksi & Ketting, 1996). Besides the success of the Challenger crawler tractors, other types of rubber tracks are also being pursued for improved tractor construction. It is still too early to reach a conclusion whether the friction driven tracks used on the Challenger series is superior to the positive drive rubber track with sprocket as developed by Bridgestone.

As can be seen from the above review, the previous research was mainly concentrating on the comparison of performance for the rubber tracks and conventional traction devices. Further research needs to be done on the prediction of performance and traction modelling to develop a better understanding of the traction mechanism and to guide further improvement of the design for rubber tracks if they are to be utilized on a larger scale.

2.5 MEASUREMENT OF THE DISTRIBUTION OF CONTACT AND TANGENTIAL STRESSES BELOW A TRACK

2.5.1 Track link dynamometer by Wills (1963)

In order to verify the assumptions of different contact pressure distributions, Wills designed and built a cantilevered dynamometer beam as shown in Figure 2.17. By the application of strain gauge transducers, the distribution and magnitude of the contact pressure and horizontal shear force below a steel track was measured simultaneously. The results in sand for different distribution types were also compared.

The results from Will's research work are currently still cited by many researchers.

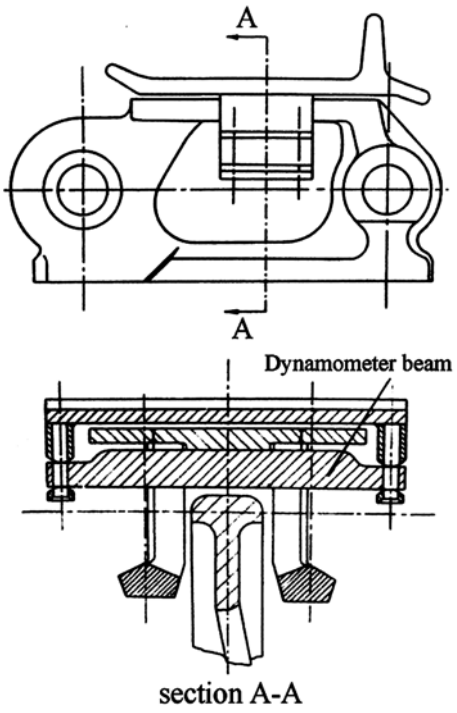

Figure 2.17. Track link dynamometer by Wills (1963).

2.5.2 Applications of extended octagonal ring transducers for measuring two perpendicular forces

The principle of the circular ring is used as the basis for the measurement of two orthogonal forces in its plane of symmetry (Lowen & Cook, 1956). As shown in Figure 2.18, with the circular ring and the properly arranged strain gauge bridge circuits, it is possible to measure the two orthogonal forces P and F independently. The octagonal form of the ring (Figure 2.18, top right) results in greater stability for the measurement of both forces. The most useful form is obtained by extending the octagonal ring by $2L_o$ (Figure 2.18, bottom). The extended octagonal ring ensures sufficient stability for most practical applications. It also minimizes the bending effects and maintains as nearly as practicable the condition of zero rotation of the top surface. The extended octagonal ring transducers have been used in agricultural engineering by many researchers (Godwin, 1975; O'Dogherty, 1975; Thakur & Godwin, 1988; Girma, 1989).

In Figure 2.18, the strain and stress at the inside and the outside surfaces of the ring due to the forces P and F are zero at θ=nodal angles, ϕ_P and ϕ_F respectively. With the strain gauges mounted in these positions and connected into the Wheatstone bridge circuits, the gauges 1-4 will measure the force F, eliminating the influence of the force P, while the gauges 5-8 will measure the force P, eliminating force F.

Although no exact solutions exists for the strain of an extended octagonal ring, the following approximate equations were suggested by O'Dogherty (1996) to predict the value of the strain caused by force P and F respectively:

Force P:

$$\varepsilon_{90^\circ} = \frac{k_P P r_o}{E b_o t_o^{\,2}} \tag{2.46}$$

Force F:

$$\varepsilon_{\phi_f} = \frac{k_F F r_o}{E b_o t_o^{\,2}} \tag{2.47}$$

In equation (2.46), k_P is the constant for P, in practice ranging from 1.50 to 1.78 with a mean value of 1.70. In equation (2.47), k_F is the constant for F, ranging from 1.66 to 2.02 with mean value of 1.80, while ϕ_P is the nodal angle at which stress, due to force P is zero. The value of ϕ_P ranges from 34° to 50° according to various researchers. For a specific application ϕ_P rather needs to be determined by calibration. E is the modulus of elasticity of the ring material.

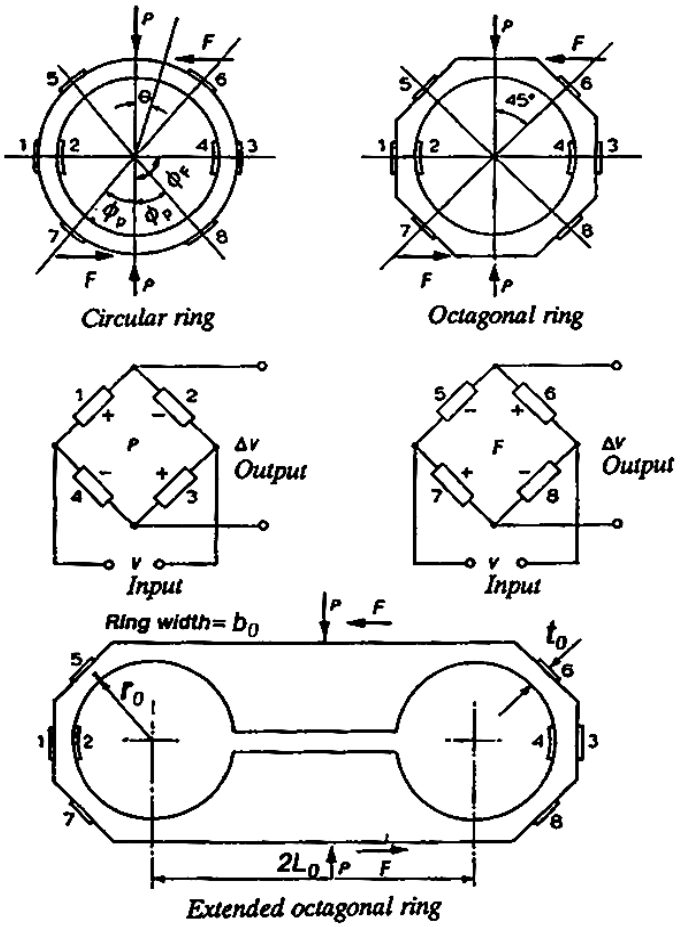

Figure 2.18. The Extended octagonal ring transducer (Godwin, 1975)

2.6 DEVELOPMENT OF THE PROTOTYPE TRACTION SYSTEM BASED ON SOIL-RUBBER FRICTION

A rubber-surfaced and friction-based track system, initially named a Bi-pole traction system (two pole wheels used at the ends of the oval track), was developed and mounted on a prototype tractor based on a new Allis Chalmers four-wheel drive tractor (Barnard, 1989).

As described by du Plessis (1996), the prototype traction concept was invented to have the terrain effect of a very large diameter wheel (Figure 2.19). This was achieved by

constructing an articulated beam type track which resists inward articulation, but allows outward articulation carried by two pairs of pneumatic wheels (N) for each track.

By using the middle wheels (M) on the track, the tractor was also expected to have significantly reduced steering resistance and damage to the ground surface when steered (Figure 2.19). It offers the additional advantage that the individual track elements can easily be replaced at low cost when compared to damaged rubber belt tracks. As the prototype track represents an alternative principle to achieve the same characteristics as the rubber belt tracks, it has the potential to be competitive to other similar mechanisms.

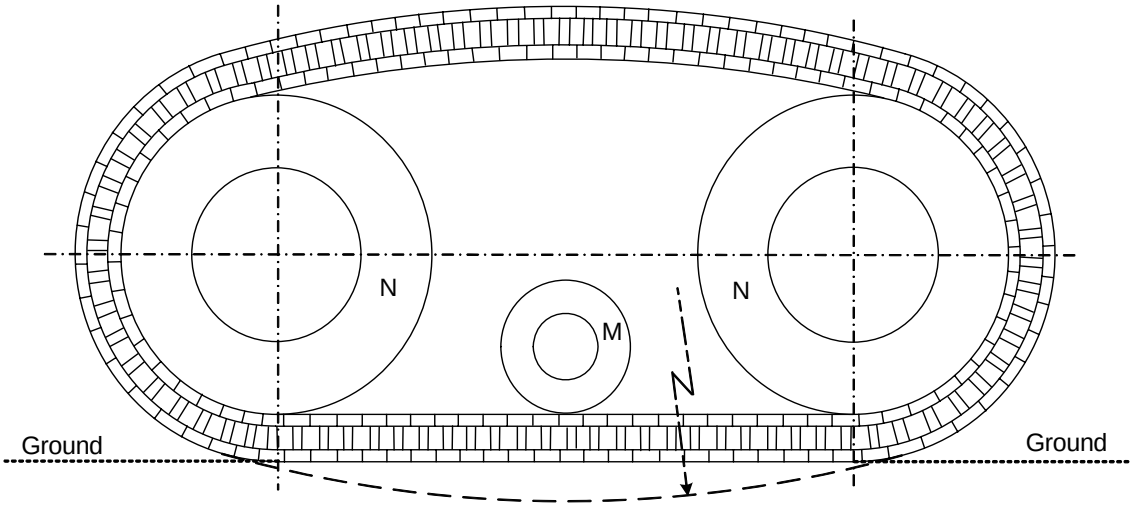

Figure 2.19. The construction concept of the prototype track to achieve the effect of a very large diameter wheel.

The initial field performance tests for the tractor equipped with this prototype track system proved that the maximum drawbar pull and power on a concrete surface at a chosen speed was notably higher than for the equivalent four-wheel drive tractor (du

Plessis, 1996). Other performance parameters were also enhanced by the prototype tracks as summarized in the report (Barnard, 1989).

2.7 JUSTIFICATION FOR CONDUCTING THIS STUDY

The literature review indicates that extensive information has been published on the subject of vehicle-terrain interaction, especially the analytical approaches pioneered by Bekker. However, there is no idealized universal approach to adequately predict and evaluate the new traction device. There is also very limited literature available for in depth research about rubber tracks.

The utilization of the rubber tracks is still in the early and rapidly developing stage (Evans and Gove, 1986. ASAE, 1995). Extensive efforts need to be made for improving the design principle of rubber tracks. It is obvious that any research and study work on this newly developed traction device would be beneficial and valuable to the future design of the traction device.

The reviewed literature has led to the following proposed approach for this study undertaken:

- The bevameter technique is a realistic approach to characterize the soil properties for analytical traction modelling.

- Based on the previous study, an analytical model to predict the contact pressure distribution below the track, as well as the tangential stress, will be derived.

- The measurement of vertical contact pressure and the tangential stress was done some years ago. The extended octagonal ring transducers are suitable to measure the vertical and the horizontal forces on the track elements.

- The shape of the terrain contact surface of the prototype track is different from that of previous traction devices. Thus the rationale of such a traction system needs to be evaluated for further improvement.

- From Neal's research (1966), it was indicated that in sandy soils, where the values of rubber-soil friction coefficient were similar to the values of the coefficient of soil internal shear resistance, the performance of a friction-based traction device such as the prototype track in this research was expected to be almost similar to that of shear-based traction device, i. e. the traditional steel tracks or wheels.

- According to the research by Wills (1963) as shown in Figure 2.14, the contact pressure distribution had a noticeable effect on the development of tractive effort, particularly at low values of slip when the tractor was usually operated. It was preferred to keep the pressure distribution in the pattern that the magnitude of the pressure at the rear end was maximum whilst at the front end the pressure was close to zero.

- The prototype track system designed by Barnard (1989) based on frictional principle was expected to have comparable tractive performance to the performance of a traditional steel track system.

2.8 OBJECTIVES

After the above literature review, the specific objectives of this study were:

- to develop an appropriate analytical model to predict the drawbar performance for the prototype track based on the friction-shear principle between rubber and soil on a soft terrain surface;

- to build the necessary measurement and instrumentation system to acquire the distribution of the contact and the tangential stresses under the prototype track;

- to measure the required soil and rubber characteristics necessary for traction modelling;

- to undertake the field tests for validation of the data from the traction modelling and the experiments under various soil conditions;

- to evaluate the effects of the design features of the prototype traction system on the tractive performance; and

- to proof that the performance of a shear-based and a friction-based traction mechanism is almost similar.

The soil parameters required for the development of the analytical model were obtained by using the instrumented apparatus applying the bevameter technique. Particularly, the characterization of the rubber-soil friction and shear were undertaken by using a standard track element. A computerized data acquisition system was used to record all the *in situ* test results for the soil characterization and the full size drawbar tests.

The special transducers to measure the distribution of the contact pressure and the friction-shear stress were built according to the principle of the extended octagonal ring. The structure of the prototype track was modified to accommodate the installation of these transducers.

After the validation of the results from the field tests and the modelling, some design features such as the frictional drive principle, the track tensioning and the function of the middle wheels were evaluated.

Figure 2.20 shows the flow chart of the procedure by which the above objectives were achieved.

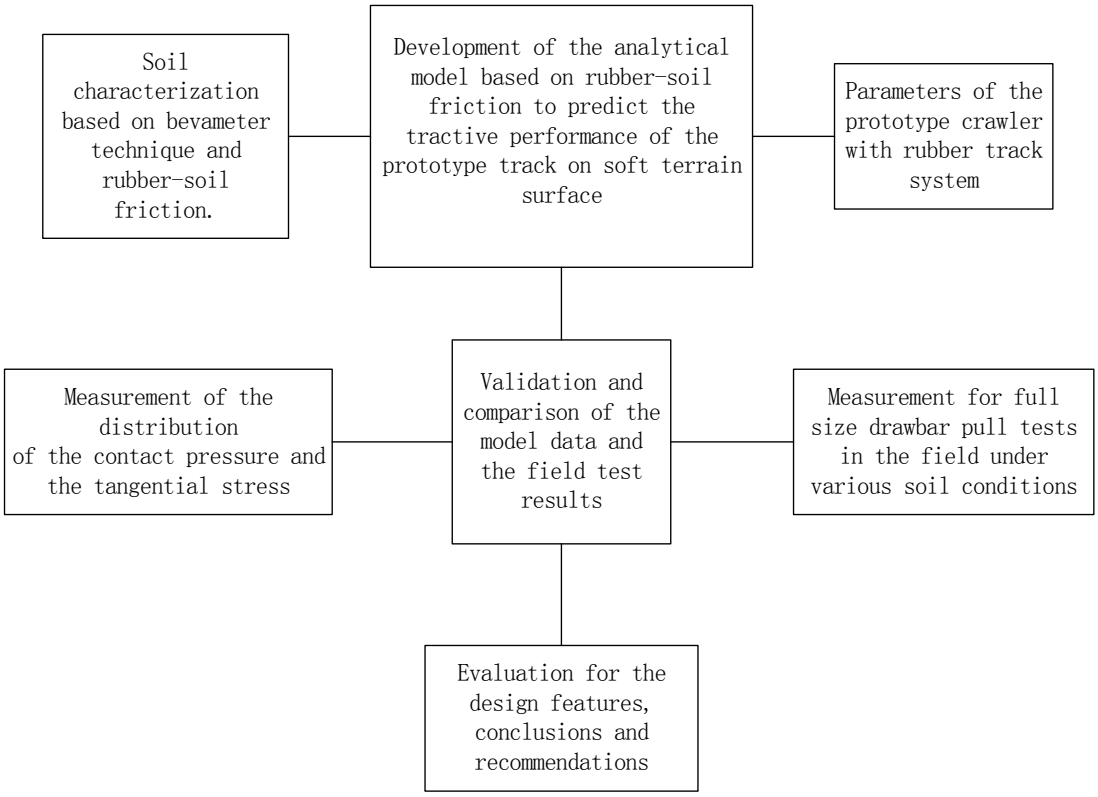

Figure 2.20. Flow chart of the proposed research procedure.